Isolation of the Magic-Size CdSe Nanoclusters [(CdSe)$_{13}$(*n*-octylamine)$_{13}$] and [(CdSe)$_{13}$(oleylamine)$_{13}$]**

Yuanyuan Wang, Yi-Hsin Liu, Ying Zhang, Fudong Wang, Paul J. Kowalski, Henry W. Rohrs, Richard A. Loomis, Michael L. Gross, and William E. Buhro

(CdSe)$_{13}$ nanoclusters have been recently reported as intermediates in the synthesis of CdSe quantum belts (nanoribbons).[1,2] We now demonstrate that a lamellar intermediate phase[1] collected from the quantum-belt synthesis is [(CdSe)$_{13}$(*n*-octylamine)$_{13}$], the smallest, discrete, magic-size nanocluster of CdSe that has been observed.[3] Kinetic data show that free, soluble [(CdSe)$_{13}$(oleylamine)$_{13}$] nanoclusters are released from the insoluble [(CdSe)$_{13}$(*n*-octylamine)$_{13}$] upon ligand exchange.

Intense research activity has focused on the study of so-called "magic-size" nanoclusters of the II–VI (12–16) semiconductors[4–7] since the initial report of (CdSe)$_{33}$ and (CdSe)$_{34}$ formation in 2004.[8] The synthetic efforts to date have generated only mixtures of magic-size CdSe nanoclusters,[9–11] and the isolation of a discrete, magic-size nanocluster has not been achieved prior to this report. We note that the carbon-fullerene field expanded dramatically following the isolation of C$_{60}$,[12] and propose that related advances for II–VI nanoclusters may now be possible. Access to purified (CdSe)$_{13}$ nanoclusters should enable experimental structure solution, chemical reactivity studies, and detailed investigations of physical and spectroscopic properties.

Nanoclusters of (CdSe)$_{13}$ are generated by reaction of cadmium acetate dihydrate, [Cd(OAc)$_2$(H$_2$O)$_2$], with selenourea [H$_2$NC(Se)NH$_2$] in *n*-octylamine solvent at room temperature. It has recently been shown that combination of CdX$_2$ compounds (X = halide,[1,13] OAc[1]) with *n*-octylamine results in the spontaneous formation of lamellar mesophases consisting of CdX$_2$ layers separated by *n*-octylamine bilayers.

[*] Y. Wang, Dr. Y. H. Liu, Y. Zhang, Dr. F. Wang, Dr. H. W. Rohrs, Prof. R. A. Loomis, Prof. M. L. Gross, Prof. W. E. Buhro
Department of Chemistry, Washington University
1 Brookings Drive, St. Louis, MO 63130 (USA)
E-mail: buhro@wustl.edu

Dr. P. J. Kowalski
Bruker Daltonics, Inc.
40 Manning Road, Billerica, MA 01821 (USA)

Addition of selenourea generates a mixture of CdSe nanoclusters that converts completely into (CdSe)$_{13}$ within 2–5 h, as indicated by spectroscopic monitoring.[1] On the same timescale, a white precipitate is deposited, which we now show to be [(CdSe)$_{13}$(*n*-octylamine)$_{13}$].

We previously demonstrated that the white precipitate contained bundles of lamellae (or layers) in which the (CdSe)$_{13}$ nanoclusters were entrained (Figure 1a).[1] The UV/Vis spectrum of the material suspended in toluene (Figure 2a) exhibited the three expected absorbances at
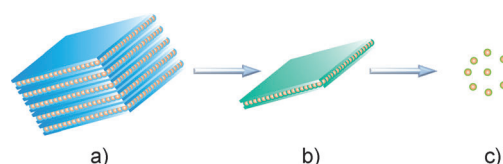

Figure 1. Disassembly of nanocluster–amine bilayer aggregates. a) Bundled nanocluster–amine bilayer aggregates from the templated synthesis of bundled [(CdSe)$_{13}$(*n*-octylamine)$_{13}$]. b) Exfoliation of colloidal sheets of aggregated nanoclusters. c) Release of freely soluble [(CdSe)$_{13}$(oleylamine)$_{13}$] nanoclusters by ligand exchange. Blue: *n*-octylamine self-assembled monolayers (a), blue-green: mixed-ligand *n*-octylamine–oleylamine monolayers (b), green: oleylamine ligand shells (c), orange: (CdSe)$_{13}$ nanoclusters.

312, 335, and 350 nm, closely matching the spectrum calculated for (CdSe)$_{13}$.[14] Note the significant scattering tail to longer wavelengths occurs, which is due to the large size of the (CdSe)$_{13}$ bundles. We also previously showed that individual layers or sheets could be exfoliated from the bundles by sonication in the presence of oleylamine (Figure 1b).[1] Figure 2a includes the UV/Vis spectrum of the exfoliated sheets dispersed in toluene. The scattering tail was absent, indicating a reduction in the dimensions of the suspended particles. Significantly, absorptions at 363, 389, and 413 nm, assigned to (CdSe)$_{19}$, (CdSe)$_{33}$, and (CdSe)$_{34}$, respectively,[1,14] were also absent, establishing the spectroscopic purity of the (CdSe)$_{13}$ obtained by the synthetic procedure.

Elemental analyses and the IR spectrum of the isolated bundles (white precipitate) established the empirical formula to be [(CdSe)(*n*-octylamine)]. Rutherford backscattering spectrometry found a Cd/Se ratio of 1.05:0.95. The CHN analyses were consistent with a CdSe/*n*-octylamine ratio of 1:1. The IR spectrum of the white precipitate showed no residual acetate or water absorptions (Supporting Information, Figure S1).

The (CdSe)$_{13}$ stoichiometry of the nanoclusters was determined by laser-desorption–ionization (LDI) mass spec-

6154

© 2012 Wiley-VCH Verlag GmbH & Co. KGaA, Weinheim
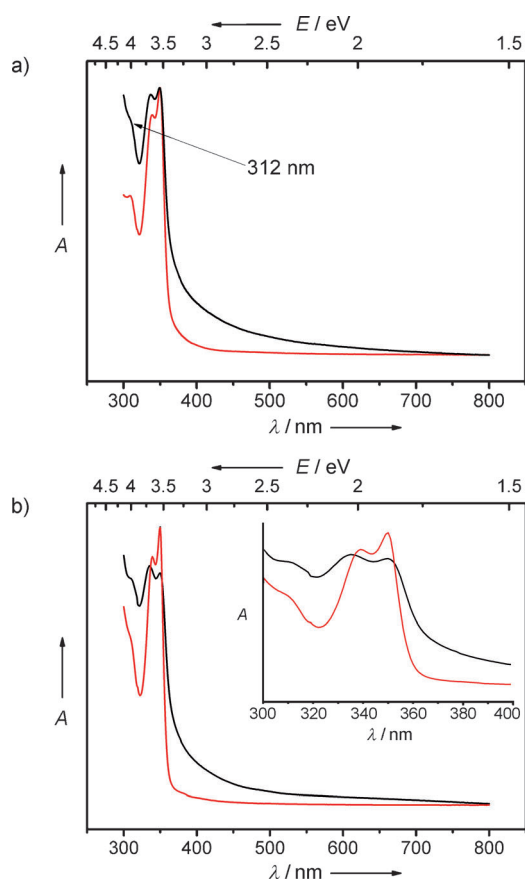
Angew. Chem. Int. Ed. **2012**, *51*, 6154–6157

Figure 2. UV/Vis spectra of $(CdSe)_{13}$. a) Spectra from bundles (black) and exfoliated sheets (red). b) Spectra from bundles and free nanoclusters. Insets: Spectral expansion to show the small spectral shift between $[(CdSe)_{13}(n\text{-octylamine})_{13}]$ bundles (black) and free $[(CdSe)_{13}(oleylamine)_{13}]$ nanoclusters (red).

trometry (Figure 3). The base peak in the spectrum appeared at m/z 2488.57, which matches the theoretical mass of $(CdSe)_{13}$. The results indicated that the *n*-octylamine ligands were detached by the LDI excitation. Small, higher-mass peaks also appeared at m/z 3638.12, 6318.03, and 6507.51 corresponding to $(CdSe)_{19}$, $(CdSe)_{33}$, and $(CdSe)_{34}$, respectively. However, LDI delivers significant energy to a sample, and we assert that the small quantities of $(CdSe)_{19}$, $(CdSe)_{33}$,

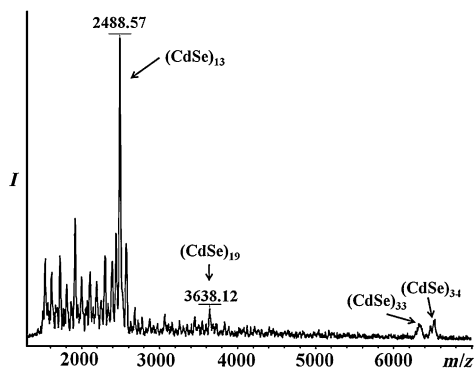**Figure 3.** LDI mass spectrum of $[(CdSe)_{13}(n\text{-octylamine})_{13}]$ bundles. Various $(CdSe)_n$ nanocluster features are labeled.

and $(CdSe)_{34}$ observed in the mass spectrum resulted from thermal heating and subsequent growth of $(CdSe)_{13}$. As noted above and shown in Figure 2a, the absorption features of these larger nanoclusters were not detected in the UV/Vis spectra of the bundled or exfoliated $(CdSe)_{13}$-containing material. We note that the spectrum in Figure 3 contrasts markedly from those published previously for mixtures of magic-sized CdSe nanoclusters[8] in that the peak for $(CdSe)_{13}$ is by far the most predominant; those for $(CdSe)_{19}$, $(CdSe)_{33}$, and $(CdSe)_{34}$ are very weak by comparison.

An expansion around the base peak at m/z 2488.57 (Figure 4a) revealed the isotopic distribution in the $(CdSe)_{13}$ nanoclusters, which was compared to the simulated isotopic distribution for $(CdSe)_{13}$ (Figure 4b). The two patterns match

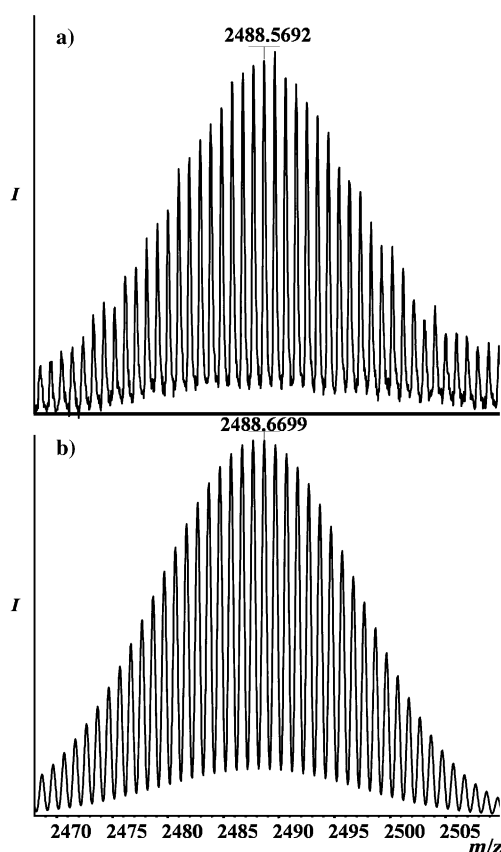**Figure 4.** Isotope distribution pattern from the mass spectrum of $(CdSe)_{13}$. a) Experimental data obtained by expansion of the spectrum in Figure 3. b) Pattern simulated using natural isotopic abundances.

closely, further confirming the $(CdSe)_{13}$ stoichiometry of the nanoclusters. The combination of the UV/Vis spectrum matching the theoretical prediction for $(CdSe)_{13}$,[14] the elemental analyses confirming the empirical formula $[(CdSe)(n\text{-octylamine})]$, and the LDI mass spectrum dominated by $(CdSe)_{13}$ establishes the white precipitate obtained from the synthesis to have the molecular formula $[(CdSe)_{13}(n\text{-octylamine})_{13}]$. The structures of $(CdSe)_{13}$ or $[(CdSe)_{13}(n\text{-alkylamine})_{13}]$ have not been experimentally determined. However, theoretical studies have found that $[(CdSe)_x(NH_3)_x]$

nanoclusters exhibit cage-like structures with one NH_3 ligand bound to each Cd atom.[15]

The sonication of mixtures of $[(CdSe)_{13}(n\text{-octylamine})_{13}]$ in toluene with an excess of oleylamine (oleylamine/$(CdSe)_{13}$ 20:1) resulted in the dissolution of $[(CdSe)_{13}(n\text{-octylamine})_{13}]$ and the release of free $[(CdSe)_{13}(oleylamine)_{13}]$ nanoclusters into solution (Figure 1 c). As described above, sonication of $[(CdSe)_{13}(n\text{-octylamine})_{13}]$ bundles (Figure 5 a,b) in oleyl-

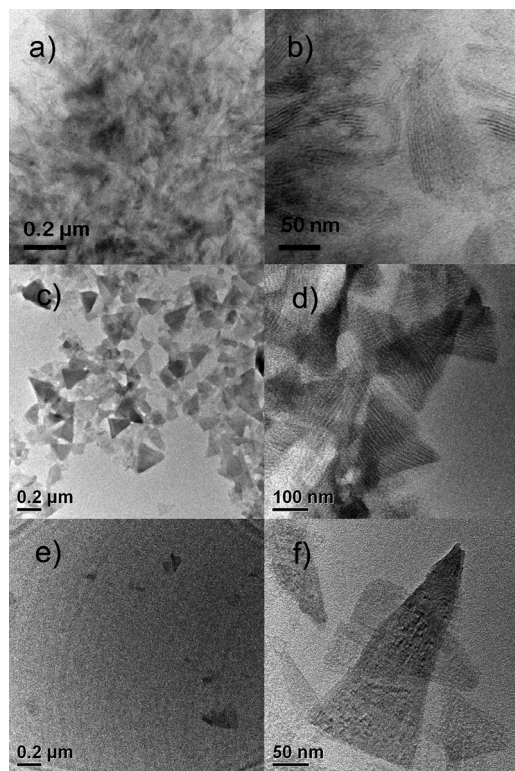*Figure 5.* TEM images of $(CdSe)_{13}$ in its various forms. a), b) Bundled $[(CdSe)_{13}(n\text{-octylamine})_{13}]$; note the lamellar features evident in (b). c), d) Exfoliated $[(CdSe)_{13}(n\text{-octylamine})_x(oleylamine)_{13-x}]$ sheets; note the striped domain pattern in (d). e), f) Residual sheets after ligand exchange and release of freely soluble $[(CdSe)_{13}(oleylamine)_{13}]$; note the lack of striped domains in (f).

amine–toluene mixtures initially exfoliated nanosheets of $[(CdSe)_{13}(n\text{-octylamine})_x(oleylamine)_{13-x}]$ (Figure 5 c,d), in which some ligand exchange was presumed to have occurred (Figure 1 b).[13] Extended sonication resulted in the destruction of the sheet structures (Figure 5 e,f), whereas the $(CdSe)_{13}$ nanoclusters remained intact, as evidenced by the retention of their characteristic absorption features (Figure 2 b). During this procedure, the initially cloudy suspension was converted into a clear solution (Supporting Information, Figure S2).

The inset in Figure 2 b is a spectral expansion in the region of the $(CdSe)_{13}$ absorbances, showing a slight shift of the 335 nm feature to 339 nm as a result of the ligand exchange. The $[(CdSe)_{13}(oleylamine)_{13}]$ stoichiometry was confirmed by elemental analysis. $[(CdSe)_{13}(oleylamine)_{13}]$ was also prepared directly from cadmium acetate dihydrate and selenourea in oleylamine (see the Supporting information).

Consequently, sonication and ligand exchange afforded a means of solubilizing the $(CdSe)_{13}$ nanoclusters.

We sought further confirmation of the formation of free, soluble $[(CdSe)_{13}(oleylamine)_{13}]$ nanoclusters from nanocluster-growth kinetics. The $[(CdSe)_{13}]$ bundles, sheets, and free nanoclusters were stable at room temperature in the solid state, in dispersion, or in solution for at least six months. However, addition of MeOH to dispersions of bundled $[(CdSe)_{13}(n\text{-octylamine})_{13}]$ (Figure 1 a), partially ligand-exchanged $[(CdSe)_{13}(n\text{-octylamine})_x(oleylamine)_{13-x}]$ nanosheets (Figure 1 b), and free $[(CdSe)_{13}(oleylamine)_{13}]$ nanoclusters (Figure 1 c) resulted in the loss of the characteristic UV/Vis absorptions at 335 and 350 nm with the appearance of a broad envelope of features at longer wavelengths (Supporting Information, Figure S3), which is consistent with indiscriminate growth of the $(CdSe)_{13}$ nanoclusters. Presumably, substitution of the small ligand MeOH for n-octylamine reduced the steric protection of the nanoclusters, allowing their coalescence and growth.

We reasoned that the steric protection of the $(CdSe)_{13}$ nanoclusters should be greatest in the $(CdSe)_{13}$ bundles and sheets (Figure 1 a,b), and least in the free nanoclusters (Figure 1 c). Consequently, the MeOH-induced growth kinetics should distinguish aggregated and free nanoclusters. The growth rate was expected to be significantly faster for the free nanoclusters, and thus a faster experimentally determined growth rate would provide strong secondary verification for the release of free, soluble nanoclusters from the bundled and sheet materials.

The methanol-induced growth of $(CdSe)_{13}$ was monitored by the decreasing absorbance of the UV/Vis feature at 350 nm in the presence of a large excess of MeOH (Supporting Information, Figure S3). The disappearance of bundled $[(CdSe)_{13}(n\text{-octylamine})_{13}]$ followed pseudo first-order kinetics over four half-lives ($k_{obs} = (1.64 \pm 0.12) \times 10^{-3}$ s^{-1}, $t_{1/2} = (423 \pm 31)$ s; Figure 6). Similarly, the disappearance of $[(CdSe)_{13}(n\text{-octylamine})_{13}]$ in the sheet structures followed
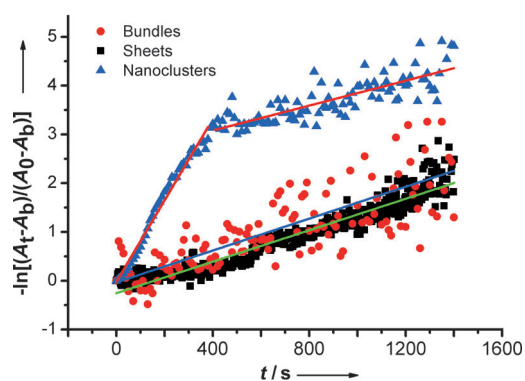

Figure 6. Kinetic data from the methanol-induced growth of $(CdSe)_{13}$. The pseudo first-order plots were constructed by monitoring the $(CdSe)_{13}$ absorbance at 350 nm, where A_t is the absorbance at time t, A_0 is the absorbance at $t = 0$ s, and A_b is the background absorbance measured at $t = 1800$ s. The slopes were extracted by linear least-squares fitting. ● ,—— Bundled $[(CdSe)_{13}(n\text{-octylamine})_{13}]$; ■ ,—— exfoliated $[(CdSe)_{13}(n\text{-octylamine})_x(oleylamine)_{13-x}]$ sheets; ▲ ,—— free $[(CdSe)_{13}(oleylamine)_{13}]$ nanoclusters.

pseudo first-order kinetics with an identical rate constant within error ($k_{obs} = (1.61 \pm 0.02) \times 10^{-3}$ s^{-1}, $t_{1/2} = (430 \pm 5)$ s; Figure 6). In contrast, the kinetic data for the disappearance of free [(CdSe)$_{13}$(oleylamine)$_{13}$] contained two pseudo first-order regimes. The initial, fast regime corresponded to $k_{obs} = (8.35 \pm 0.20) \times 10^{-3}$ s^{-1} ($t_{1/2} = (83 \pm 2)$ s; Figure 6), which is five times faster than the growth rates of (CdSe)$_{13}$ in the bundles and sheets. The second, slow regime corresponded to $k_{obs} = (1.68 \pm 0.03) \times 10^{-3}$ s^{-1} ($t_{1/2} = (413 \pm 7)$ s; Figure 6), which is indicative of the residual sheet-like structures in the specimen (Figure 5b). Because the initial, fast regime persisted over three decades in concentration, we estimate the quantity of residual, aggregated (CdSe)$_{13}$ to be $\leq 0.1\%$. Thus, the kinetic results strongly supported the liberation of free, soluble [(CdSe)$_{13}$(oleylamine)$_{13}$] nanoclusters from the aggregated bundles and sheets.

Addition of 2-propanol or acetone also induced the growth of [(CdSe)$_{13}$(oleylamine)$_{13}$]. Kinetic data collected under pseudo first-order conditions as a function of additive concentration established that the growth processes were first order in additive, for MeOH (Supporting Information, Figure S4), 2-propanol (Supporting Information, Figure S5), and acetone (Supporting Information, Figure S6). Assuming that growth is triggered by the substitution of the smaller additive ligands for oleylamine ligands, the first-order nature of the kinetics in additive suggests that the first ligand substitution is rate-determining. Apparently, loss of the first oleylamine ligand compromises the steric protection of the nanocluster ligand shell, promoting rapid substitution of the remaining oleylamine ligands and subsequently allowing coalescence and growth of the (CdSe)$_{13}$ nanoclusters.

The fact that the syntheses reported here provide (CdSe)$_{13}$, exclusive of nanoclusters of other sizes, is surprising. However, spectroscopic monitoring established the initial formation of mixtures of (CdSe)$_{13}$, (CdSe)$_{19}$, (CdSe)$_{33}$, and (CdSe)$_{34}$, which ultimately equilibrate to (CdSe)$_{13}$.[1] The results strongly suggest that (CdSe)$_{13}$ is the most thermodynamically stable nanocluster within the amine bilayer template (Figure 1a) in which it forms.[1] The results further suggest that subsequent liberation by oleylamine ligand exchange produces sterically protected, free (CdSe)$_{13}$ nanoclusters that are kinetically stabilized. After the steric protection is compromised by small-ligand substitution with methanol, 2-propanol, or acetone, the nanoclusters prefer to grow to larger sizes, which are more stable outside of the synthetic template. In summary, discrete, magic-size (CdSe)$_{13}$(n-alkylamine)$_{13}$ nanoclusters have been prepared and isolated, and are thus now available for further studies.

[1] Y. H. Liu, F. Wang, Y. Wang, P. C. Gibbons, W. E. Buhro, *J. Am. Chem. Soc.* **2011**, *133*, 17005–17013.

[2] J. H. Yu, X. Y. Liu, K. E. Kewon, J. Joo, J. Park, K. T. Ko, D. W. Lee, S. P. Shen, K. Tivakornsasithorn, J. S. Son, J. H. Park, Y. W. Kim, G. S. Hwang, M. Dobrowolska, J. K. Furdynal, T. Hyeon, *Nat. Mater.* **2010**, *9*, 47–53.

[3] H. S. Kim, S. W. Jang, S. Y. Chung, S. Lee, Y. H. Lee, B. S. Kim, C. Liu, D. Neuhauser, *J. Phys. Chem. B* **2010**, *114*, 471–479.

[4] M. J. Bowers II, J. R. McBride, S. J. Rosenthal, *J. Am. Chem. Soc.* **2005**, *127*, 15378–15379.

[5] B. M. Cossairt, J. S. Owen, *Chem. Mater.* **2011**, *23*, 3114–3119.

[6] F. S. Riehle, R. Bienert, R. Thomann, G. A. Urban, M. Kruger, *Nano Lett.* **2009**, *9*, 514–518.

[7] G. D. Scholes, *Nat. Mater.* **2011**, *10*, 906–907.

[8] A. Kasuya, R. Sivamohan, Y. A. Barnakov, I. M. Dmitruk, T. Nirasawa, V. R. Romanyuk, V. Kumar, S. V. Mamykin, K. Tohji, B. Jeyadevan, K. Shinoda, T. Kudo, O. Terasaki, Z. Liu, R. V. Belosludov, V. Sundararajan, Y. Kawazoe, *Nat. Mater.* **2004**, *3*, 99–102.

[9] A. D. Dukes, J. R. McBride, S. J. Rosenthal, *Chem. Mater.* **2010**, *22*, 6402–6408.

[10] S. Kudera, M. Zanella, C. Giannini, A. Rizzo, Y. Q. Li, G. Gigli, R. Cingolani, G. Ciccarella, W. Spahl, W. J. Parak, L. Manna, *Adv. Mater.* **2007**, *19*, 548–552.

[11] Y. Noda, H. Maekawa, A. Kasuya, *Eur. Phys. J. D* **2010**, *57*, 43–47.

[12] W. Krätschmer, L. D. Lamb, K. Fostiropoulos, D. R. Huffman, *Nature* **1990**, *347*, 354–358.

[13] J. S. Son, X. D. Wen, J. Joo, J. Chae, S. I. Baek, K. Park, J. H. Kim, K. An, J. H. Yu, S. G. Kwon, S. H. Choi, Z. W. Wang, Y. W. Kim, Y. Kuk, R. Hoffmann, T. Hyeon, *Angew. Chem.* **2009**, *121*, 6993–6996; *Angew. Chem. Int. Ed.* **2009**, *48*, 6861–6864.

[14] M. D. Ben, R. W. A. Havenith, R. Broer, M. Stener, *J. Phys. Chem. C* **2011**, *115*, 16782–16796.

[15] K. A. Nguyen, P. N. Day, R. Pachter, *J. Phys. Chem. C* **2010**, *114*, 16197–16209.